Driver-in-the-Loop Testing of Genetic Algorithm-Tuned Active Anti-Roll Bar for Vehicle Lateral Stability

Samuel Sonnino[1], Stefano Melzi[1], Francesco Pirchio[1], Raffaele Verde[1], Pietro Caresia[2], Alessandro Manzoni[2], Gianluca Vaini[2]

(1) Politecnico di Milano, {samuel.sonnino, stefano.melzi}@polimi.it
(2) Brembo N.V., {pietro.caresia, alessandro.manzoni, gianluca.vaini}@brembo.com

Abstract - *This study presents the assessment of an Active Anti-Roll Bar (AARB) system using a driving simulator, aiming to enhance vehicle lateral stability and overall handling performance. The research focuses on optimizing the control strategy through a genetic algorithm and evaluating its effectiveness via offline simulations and Driver-in-the-Loop (DiL) testing, utilizing a 14-degree-of-freedom vehicle model from VI-CarRealTime. The proposed AARB system dynamically adjusts the roll stiffness of the front and rear axles, effectively reducing body roll and improving stability during high-speed maneuvers. The results highlight significant improvements in mitigating understeer and oversteer, enhancing both driver confidence and vehicle safety. The findings indicate that integrating genetic algorithms for control tuning, combined with real-time validation through DiL testing, offers a robust approach to advancing vehicle dynamics control systems.*

Keywords: *Active Anti-Roll Bar, Vehicle Lateral Stability, Genetic Algorithm, Control Tuning, Driver-In-The-Loop*

Introduction

The Active Anti-Roll Bar (AARB) is a suspension system component designed to dynamically adjust the vehicle's roll stiffness . Unlike traditional Anti-Roll Bars (ARBs), which have a fixed torsional stiffness (Duc, Ngoc, and Thi, 2022), AARB system can enhance comfort, lateral stability and vehicle responsiveness by actively adapting its stiffness to match current driving conditions (Nguyen, 2021; Sagewka, et al., 2017).

In vehicle dynamics, the distribution of roll stiffness between the front and rear axles, known as Roll Stiffness Distribution (RSD), plays a pivotal role in shaping the vehicle's handling characteristics (Pacejka, 2005). Achieving the right balance is crucial for maintaining predictable and safe handling, particularly during high lateral acceleration conditions where load transfer effects become significant.

This study focuses on optimizing the control logic of the AARB system using a genetic algorithm (GA) to improve vehicle lateral dynamics. The system's effectiveness is validated through extensive offline simulations and Driver-in-the-Loop (DiL) testing on a group of volunteers using the Cable-Driven Dynamic Driving simulator of $Politecnico\ di\ Milano$.

Control Logic

The AARB system is designed to actively control the roll stiffness of the front and rear axles by employing a combination of feedforward and feedback contributes. Figure 1 illustrates the block diagram of the AARB control logic, highlighting the major components:

- Feedforward Stiffness Contribution
- Yaw Rate Reference Generation
- Feedback Stiffness Contribution
- AARB Actuation Model

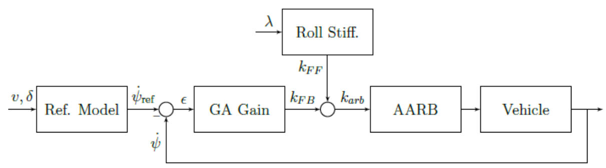

Figure 1: Block diagram of the control logic

Feedforward Contribution

The feedforward contribution establishes the baseline AARB roll stiffness, k_{FF} by scaling the total anti-roll bar base stiffness using a coefficient λ.
The additional stiffness values, $k_{\text{add},f}$ and $k_{\text{add},r}$ are specifically computed to preserve the vehicle's original RSD by solving the following system of equations:

$$\begin{cases} RSD = \frac{k_{\text{susp},f}+k_{\text{arb},f}+k_{\text{add},f}}{k_{\text{susp},f}+k_{\text{arb},f}+k_{\text{add},f}+k_{\text{susp},r}+k_{\text{arb},r}+k_{\text{add},r}} \\ k_{\text{arb},f}+k_{\text{add},f}+k_{\text{arb},r}+k_{\text{add},r} = (k_{\text{arb},f}+k_{\text{arb},r})\cdot\lambda \end{cases} \tag{1}$$

Where $k_{\text{susp,f}}$ and $k_{\text{susp,r}}$ represent the suspension roll stiffness at the front and rear axles respectively, λ

the percentage increase of ARBs roll stiffness, while $k_{\text{arb,f}}$ and $k_{\text{arb,r}}$ denote the baseline roll stiffness of the anti-roll bars at the front and rear axles respectively.

The final feedforward AARB stiffness contribution for the i-th axle is thus given by:

$$k_{\text{arb,FF},i} = k_{\text{arb},i} + k_{\text{add},i} \tag{2}$$

Feedback Contribution

The feedback component of the AARB system aims to improve the stability of the vehicle by minimizing the yaw rate error (ϵ) defined as:

$$\epsilon = |\dot{\psi}_{\text{ref}}| - |\dot{\psi}| \tag{3}$$

where is $\dot{\psi}$ is the actual yaw rate of the vehicle measured in real-time.

The yaw rate reference ($\dot{\psi}_{\text{ref}}$) is derived using a 2-DoF single-track vehicle model (Schramm, Hiller, and Bardini, 2014; Mastinu and Plöchl, 2014). Since this reference apply a linear relationship between yaw rate and steering angle a transition to an exponential decay model is implemented to express tire saturation (Asperti, Vignati, and Sabbioni, 2024).
The equations used are:

$$\dot{\psi}_{\text{ref}} = \begin{cases} \frac{v}{l(1+K_{\text{us}}v^2)}\delta = \alpha\delta & \text{if } \delta \leq \delta^* \\ \dot{\psi}_{\text{max}} + \left(\dot{\psi}^* - \dot{\psi}_{\text{max}}\right) e^{\frac{-\alpha(\delta-\delta^*)}{(\dot{\psi}_{\text{max}}-\dot{\psi}^*)}} & \text{if } \delta > \delta^* \end{cases} \tag{4}$$

Where K_{us} is the understeer gradient, v the longitudinal velocity of the vehicle, δ the front steering angle, m the vehicle mass, l the wheelbase, l_f and l_r the CoG distance from front/rear axle, C_{α_f} and C_{α_r} the cornering stiffness, and μ the road friction coefficient.

The feedback stiffness contributions for the front and rear anti-roll bars are thus computed as:

$$\begin{aligned} k_{\text{FB},r} &= G_i \cdot \epsilon \\ k_{\text{FB},f} &= -G_i \cdot \epsilon \end{aligned} \tag{5}$$

where the sign of the error ϵ determines whether the stiffness is added or subtracted from $k_{\text{FF},i}$.

The control gain, G_i, assumes two distinct values, G_{us} and G_{os}, based on the vehicle's handling scenario detected (understeering or oversteering). This approach provides finer control tuning, tailored to the characteristics of the baseline vehicle.
The total AARB roll stiffness applied to the i-th axle is then given by:

$$k_{\text{arb},i} = k_{\text{FF},i} + k_{\text{FB},i}, \tag{6}$$

Actuator Dynamics Modeling

The dynamics of the actuators in the AARB control system are modeled using a first-order filter in order to captures system delays and smooth out high-frequency inputs:

$$H(s) = \frac{1}{\tau s + 1} \tag{7}$$

Where the time constant τ defines the responsiveness of the actuator.

Genetic Algorithm

The Genetic Algorithm (GA) (Holland, 1975; Katoch, Chauhan, and Kumar, 2021) framework used to optimize the control parameters G_{us} and G_{os}, consists of several key stages (Figure 2). The objective is to maximize vehicle stability and handling performance while minimizing the actuation effort.

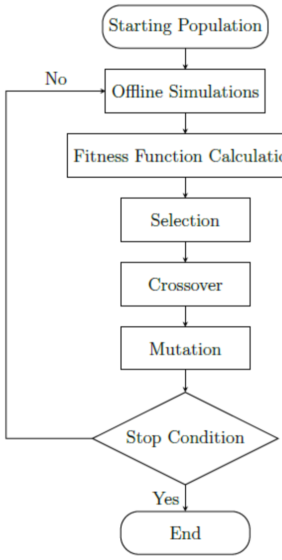

Figure 2: Flowchart of the GA

The Genetic Algorithm (GA) follows these steps:

1. **Initialization:** A population of individuals with genes G_{us} and G_{os} is randomly initialized within feasible ranges to ensure genetic diversity.
2. **Fitness Function Evaluation:** Each j-th individual is tested using a 14-DoF VI-CarRealTime model integrated with the AARB model in Simulink over the i-th ISO maneuvers (4138, 7401, 19365) at four speeds (60, 80, 100, 120 km/h).
Key metrics form KPIs used to compute handling, comfort, and actuator effort sub-fitness functions are then combined via a weighted average as:

$$\text{FF}(j) = \frac{\sum_i w_i \times ff_i(j)}{\sum_i w_i} \tag{8}$$

3. **Selection:** Individuals with higher fitness score $\text{FF}(j)$ are more likely to be selected as parents for the next generation.
4. **Crossover:** Combines genetic material from two parent individuals to produce offspring. This mechanism introduces new genetic combinations, aiding the exploration of new solutions.
5. **Mutation:** Introduces random variations in the genes of selected individuals to prevent the population from becoming too homogeneous.
6. **Termination and Iteration:** The GA runs iteratively until convergence (Figure **??**), defined by the lack of further improvements. The result is the optimal set of G_{us} and G_{os} values balancing stability, handling, and actuator effort.

Simulation Settings

Driver-in-the-Loop (DiL) testing is conducted using the high-fidelity driving simulator DIM400 of

Politecnico di Milano DriSMi (Figure 3).
Table 1 summarizes the key technical specifications and capabilities of the DriSMi Cable-Driven DIM400 Dynamic Simulator.

Figure 3: DIM400 Simulator - Politecnico di Milano

Table 1: Technical specifications of the DriSMi simulator

Feature	Specification
Platform	Size: 6x6 m platform DoFs: 9 (diskframe + hexalift)
Workspace	a_x/a_y: Up to 1.5g a_z: Up to 2.5g Vertical displacement: $\pm$ 280 mm
Bandwidth	Diskframe: $\sim$3 Hz Hexalift: $\sim$30 Hz Onboard vibration shakers: $\sim$200 Hz
Active Components	Active belt and seat Active steering and brake
Latency	Overall latency: $\sim$20 ms
Cockpit Immersion	Visual Display: 270° screen Sound System: 5 speakers

To ensure safety, operational limits were imposed on the simulator during testing: side slip angle β was capped at 0.8 rad and its rate at 1 rad/s. If exceeded, the simulation was automatically halted to prevent loss of control and protect participants from abrupt motions. For this reason, although the simulator is capable of 1:1 motion cueing, displacement and rotation filters were applied.

The testing scenario is designed within the software VI-WorldSim to replicate a double lane change (ISO3888-2) on a three-lane highway (Figure 4), a maneuver widely recognized for evaluating vehicle handling and driver response under dynamic conditions.

At the end of each corridor, an obstacle in the form of a bus is placed to enhance realism and create a greater sense of danger for drivers, thereby increasing their immersion in the hazardous scenario.

To let drivers focus solely on steering, the vehicle maintained a preset speed using cruise control, deactivated just before entering the cones. This ensured consistent test conditions and allowed accurate assessment of control system performance and driver perception.

Figure 4: Driving Scenario

Experimental Campaign

The sample group consisted of 24 participants, equally divided by gender (12 males and 12 females), aged between 19 and 29 years.
Moreover, only about 10% of participants had prior experience with a driving simulator.

Each driver was given a free practice session to familiarize themselves with the driving simulator during which they performed slalom maneuvers at various speeds within the previous highway scenario.
Following this, they were required to perform the described double lane change maneuver at three different speeds: 60 km/h, 70 km/h, and 80 km/h.
For each of these speeds, the maneuver is repeated twice: once with the vehicle in the baseline configuration and once with active anti-roll bars.

To mitigate any potential learning effect, the sequence of passive and active configurations presented to each participant was randomized.
This randomization ensured that drivers were not simply performing better due to repeated exposure to the maneuver, but rather any observed improvement could be more confidently attributed to the benefits of the active anti-roll bar system.
Furthermore, drivers were not informed about which configuration they were testing to prevent any bias or influence on their performance.

Objective Results

The data analysis conducted involves trajectories, steering angle (δ_{SW}), yaw rate ($\dot{\psi}$), and side slip angle (β) of all participants. Additionally, an average plot was created, which represented the mean response of all participants for each variable.

For brevity, only the results of the test at 70 km/h are reported below, as this speed is representative of the overall trends observed and serves as a meaningful reference for the problem under study.

Figure 5 and 6 illustrates the average trajectories of all 24 drivers and corresponding vehicle dynamics parameters respectively for the two vehicle configurations tested: Baseline and AARB.

The results show that the controlled vehicle follows a trajectory more consistent with the intended path, exhibits a smoother steering input, maintain a yaw rate

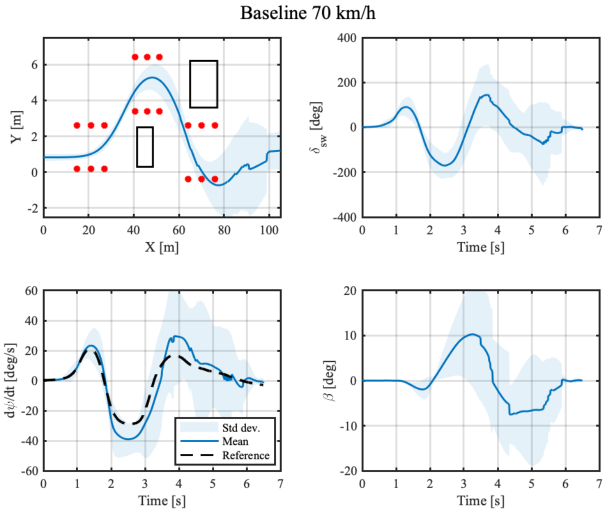

Figure 5: Baseline Vehicle at 70km/h

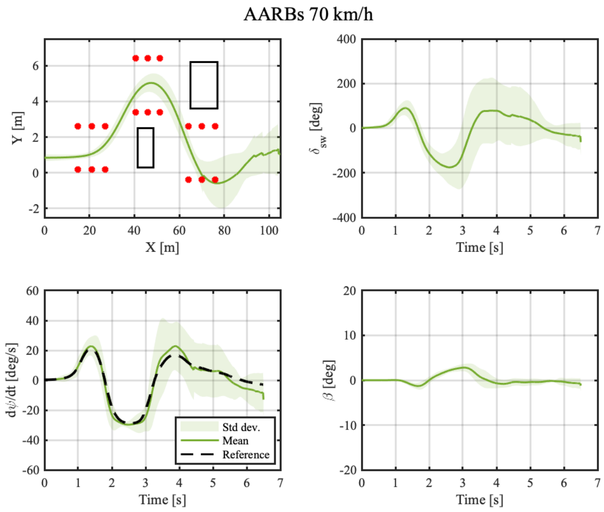

Figure 6: Controlled Vehicle at 70km/h

closer to the reference, and achieves a significantly lower side slip angle compared to the standard vehicle, indicating improved vehicle stability.

In the case of the passive vehicle, it is evident that around 3.5 seconds the first driver loses control, causing the simulation to terminate due to the predefined safety limits on side slip angle (0.8 rad) or side slip angle rate (1 rad/s). From that moment onward, the curve becomes fragmented because the sample of drivers included in the analysis changes, considering only those who are able to maintain vehicle stability within the simulator limits. This behavior does not occur with the controlled vehicle, as none of the drivers exceeded the side slip thresholds, allowing all simulations to continue until the end.

Subjective Results

At the end of each maneuver, after testing both vehicle configurations (Baseline and AARB) in a randomized order, drivers were asked which vehicle they perceived as more stable and safer during the maneuver.
Their preference for all the speed tested (60, 70, 80 km/h), is reported in Table 2.

Table 2: Number of participants preferring Baseline or AARB configurations at each speed

Speed	Configuration Preference	n. of Participants
60 km/h	Baseline	8
	AARB	16
70 km/h	Baseline	6
	AARB	18
80 km/h	Baseline	5
	AARB	19

It can be observed that as speed increases, the preference for the AARB vehicle configuration also rises, indicating that in situations where vehicle stability is more critical, active controls are favored.

Moreover, at the end of all the simulations, participants were asked to assess the extent to which they felt the control system generally contributed to successfully completing the simulated emergency maneuver as well as how intrusive they perceived the AARB's intervention. Their cross-assessments, rated on a five-point scale, are shown in Figure 7, where the number next to each marker indicates how many drivers gave that rating.

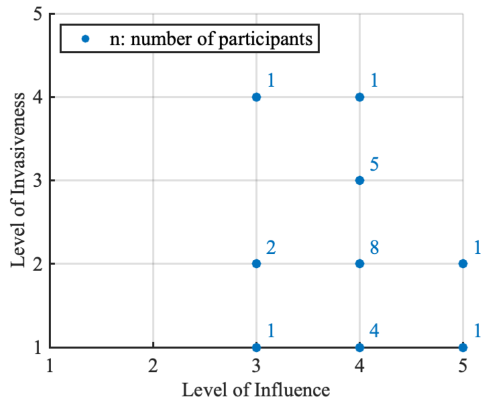

Figure 7: AARB Influence and Invasiveness

The perceived assistance provided by the control system aligns with objective performance improvements noted in trajectory and stability metrics.
The invasiveness level, on the other hand, shows that the system was well perceived and tolerated by the drivers, who gave predominantly low ratings for the level of invasiveness.

Objective and Subjective Data Correlation

Drivers' vehicle configuration preference (Baseline or AARB), rated on a five-point scale, is displayed on the x-axis of the box plot in Figure 8, while on the y-axis the objective difference between the two vehicle configuration is reported.
The difference between the maximum yaw rate achieved during the maneuver for the baseline and

controlled vehicle configuration is used as comparative index:

$$\Delta\dot{\psi} = max|\dot{\psi}_{\text{Base}}| - max|\dot{\psi}_{\text{AARB}}| \quad (9)$$

As instance, positive values of $\Delta\dot{\psi}$ indicate that the yaw rate was higher in the baseline configuration, suggesting less controlled and more unstable vehicle behavior.

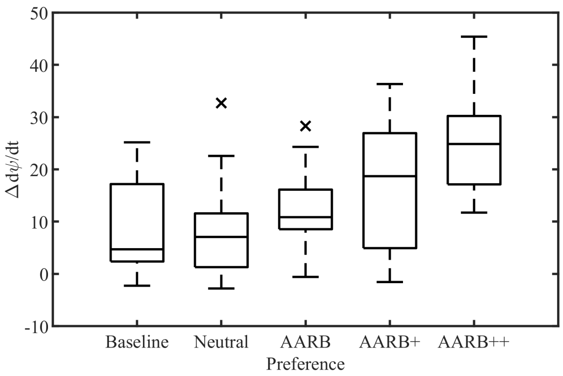

Figure 8: Boxplot for objective and subjective data correlation

The box plot reveals a clear relationship between the subjective ratings and the objective performance of the vehicle configurations:

- **Preference for Active Configuration:** Participants who preferred the active configuration consistently exhibited larger positive $\Delta\dot{\psi}$, confirming that the active system provided noticeable improvements in yaw stability.
- **Preference for Baseline Configuration:** A subset of participants who favored the baseline setup displayed smaller or even negative $\Delta\dot{\psi}$, suggesting that for these individuals, the baseline configuration either felt more natural or matched their expectations of vehicle behavior.

  However, the heterogeneous distribution of $\Delta\dot{\psi}$ for those who gave low ratings, highlights that the preference for the passive vehicle is not always correlated with worst performance with AARB. In contrast, preferences for the controlled vehicle, show greater alignment between participants ratings and the objective data.

Conclusions

This study presented the design, optimization, and evaluation of an Active Anti-Roll Bar (AARB) system aimed at improving vehicle lateral stability. By dynamically adjusting roll stiffness, the AARB overcomes the limitations of passive systems, enhancing handling and safety, especially during high-speed or emergency maneuvers.

Control gains were optimized using a Genetic Algorithm (GA) to balance stability, comfort, and actuator effort. Offline simulations with a 14-DoF vehicle model confirmed improved yaw response, stability, and predictability across scenarios.

Driver-in-the-Loop (DiL) testing at the DrisMi simulator further validated performance. Most drivers reported enhanced control and confidence during rapid lane changes, particularly at higher speeds.

In conclusion, the AARB effectively reduces understeer and oversteer by optimizing roll stiffness distribution. The GA-based tuning, validated through DiL testing, supports a robust framework for advanced vehicle dynamics control systems that improve safety, performance, and driver experience.

Acknowledgements

The authors would like to express their gratitude to the technicians of the driving simulators at Politecnico di Milano and Brembo for their support during this study.

References

Asperti, M., Vignati, M., and Sabbioni, E., 2024. On Torque Vectoring Control: Review and Comparison of State-of-the-Art Approaches. *Machines*, 12(3), p. 45.

Duc, N. N., Ngoc, D. D., and Thi, T. H. T., 2022. Effect of the Passive Stabilizer Bar on the Vehicleâs Stability.

Holland, J. H., 1975. *Adaptation in Natural and Artificial Systems*. University of Michigan Press.

Katoch, S., Chauhan, S. S., and Kumar, V., 2021. A review on genetic algorithm: past, present, and future. *Multimedia Tools and Applications*, 80, pp. 8091–8126.

Mastinu, G. and Plöchl, M., 2014. *Road and off-road vehicle system dynamics handbook*. CRC press.

Nguyen, T. A., 2021. Improving the Stability of the Passenger Vehicle by Using an Active Stabilizer Bar Controlled by the Fuzzy Method. *Complexity*, 2021, Article ID 6569298, 20 pages.

Pacejka, H., 2005. *Tire and vehicle dynamics*. Elsevier.

Sagewka, S., Fiebig, T., Schmid, C., and Wostal, D., 2017. Mechatronic Roll Control for the 48-V Electrical System. *ATZ Worldwide*, 108(11), pp. 28–33.

Schramm, D., Hiller, M., and Bardini, R., 2014. *Vehicle dynamics*. Springer.